JPET Fast Forward. Published on August 17, 2017 as DOI: 10.1124/jpet.117.243014
This article has not been copyedited and formatted. The final version may differ from this version.

JPET/2017/243014

Title: Claudin-5-binders enhance permeation of solutes across the blood–brain barrier in a mammalian model

Authors: Yosuke Hashimoto, Keisuke Shirakura, Yoshiaki Okada, Hiroyuki Takeda, Kohki Endo, Maki Tamura, Akihiro Watari, Yoshifusa Sadamura, Tatsuya Sawasaki, Takefumi Doi, Kiyohito Yagi, Masuo Kondoh

Affiliations:

Graduate School of Pharmaceutical Sciences, Osaka University, Osaka 565-0871, Japan (Y.H., K.S., Y.O., A.W., T.D., K.Y. and M.K.)

Proteo-Science Center, Ehime University, Ehime, 790-8577, Japan (H.T. and T.S.)

Life Science Research Laboratories, Wako Pure Chemical Industries, Ltd., Hyogo, 661-0963, Japan (K.E., M.T. and Y.S.)

JPET Fast Forward. Published on August 17, 2017 as DOI: 10.1124/jpet.117.243014
This article has not been copyedited and formatted. The final version may differ from this version.

a) Running title

Claudin-5 binder modulates blood–brain barrier permeability.

b) Corresponding author

Masuo Kondoh, PhD, Graduate School of Pharmaceutical Sciences, Osaka University, Suita, Osaka 565-0871, Japan; Tel: +81-6-6879-8196; Fax: +81-6-6879-8199; E-mail: masuo@phs.osaka-u.ac.jp

c)

Number of text pages: 30

Number of tables: 1

Number of figures: 5

Number of references: 48

Number of words in the Abstract: 134

Number of words in the Introduction: 604

Number of words in the Discussion: 951

d) Abbreviations: BBB, blood–brain barrier; BSA, bovine serum albumin; C-CPEmt, C-terminal half of *Clostridium perfringens* enterotoxin mutant; CLDN, claudin; CNS, central nervous system; CSF, cerebrospinal fluid; DMEM, Dulbecco's modified Eagle's medium; ECL, extracellular loop domain; FBS, fetal bovine serum; FD-4, fluorescein isothiocyanate-labeled dextran with an average weight of 4 kDa; FNa, sodium fluorescein; mAb, monoclonal antibody; PBS, phosphate-buffered saline; TEER, trans-epithelial/endothelial electrical resistance; TJ, tight junction; T-TBS, Tris-buffered

JPET Fast Forward. Published on August 17, 2017 as DOI: 10.1124/jpet.117.243014
This article has not been copyedited and formatted. The final version may differ from this version.

saline containing 0.05% Tween-20; ZO, zonula occludens.

e) A recommended section: Cellular and Molecular

JPET Fast Forward. Published on August 17, 2017 as DOI: 10.1124/jpet.117.243014
This article has not been copyedited and formatted. The final version may differ from this version.

Abstract

A current bottleneck in the development of central nervous system (CNS) drugs is the lack of drug delivery systems targeting the CNS. The intercellular space between endothelial cells of the blood brain barrier (BBB) is sealed by complex protein-based structures called tight junctions (TJs). Claudin-5, a tetra-transmembrane protein is a key component of the TJ seal that prevents the paracellular diffusion of drugs into the CNS. In the present study, to investigate whether CLDN-5 binders can be used for delivery of drugs to the CNS, we generated monoclonal antibodies specific to the extracellular domains of CLDN-5. In an *in vitro* model of the blood–brain barrier, the anti-CLDN-5 mAbs dose-dependently attenuated TEER and enhanced solute permeation. These anti-CLDN-5 monoclonal antibodies are potential leads for the development of novel drug delivery systems targeting the CNS.

Introduction

The regulatory success rate for central nervous system (CNS) drugs is less than half that of non-CNS drugs (Kaitlin, 2014). Current bottlenecks in the development of CNS drugs include delay in development of conventional experimental models to accurately predict the efficacy of drug candidates *in vivo* and a lack of drug delivery systems to efficiently deliver drugs to the CNS (Pardridge, 2005; Gribkoff and Kaczmarek, in press). Recent progress in genome editing and induced pluripotent stem cell technologies has led to the development of several experimental models useful for the development of CNS drugs (Heidenreich and Zhang, 2016; Liu and Deng, 2016; Gribkoff and Kaczmarek, in press); however, efficient delivery of drugs to the CNS remains a challenge.

The blood–brain barrier (BBB) is a membrane barrier formed by brain capillary endothelial cells that protects the brain from harmful materials circulating in the blood (Rubin and Staddon, 1999). Ninety-eight percent of small-molecule drugs and nearly all large-molecule drugs, including antibodies, recombinant proteins, and antisense therapeutics, do not readily cross the BBB (Pardridge, 2005). Drugs that readily cross the BBB do so via either transcellular transport (i.e., through cell bodies via receptors and transporters in the cell membrane) or paracellular transport (i.e., through the intercellular space between cells) (Laksitorini et al., 2014). To date, most studies aimed at enhancing the delivery of drugs across the BBB have focused on transcellular transport-based methods such as increasing the passive diffusion of drugs by altering their physicochemical properties (Betz et al., 1980; Lipinski et al., 2001) or using receptor-mediated transport and carrier proteins such as transferrin receptors (Pardridge,

2007; Pardridge and Boado, 2012).

Tight junctions (TJs) are complex biochemical structures that seal the intercellular space between adjacent endothelial cells, which prevents the diffusion of solutes from the systemic circulation into the CNS via the BBB. Thus, the strategy underlying the delivery of drugs to the brain via paracellular transport is to disrupt, or open, the TJ seal in the BBB (Pardridge, 2005). Osmotic opening of the TJ seal by injection of mannitol has been used clinically to deliver anticancer drugs directly to brain tumors, with transient adverse effects, such as the leakage of albumin into the brain, but without clinically significant adverse effects (Rapoport, 2000). In addition, phase 1/2a studies have revealed that repeated opening of the BBB by using a pulsed ultrasound system is safe and well tolerated in patients with brain tumor (Carpentier et al., 2016). However, the potential applications of this method are limited because it opens the BBB to all large molecules, not just the target drug (Laksitorini et al., 2014).

TJs are composed of transmembrane proteins (e.g., junctional adhesion molecules, occludin, claudins, tricellulin, angulins) and intracellular adaptor proteins (e.g., zonula occludens [ZO]) (Furuse, 2014; Zihni et al., 2016). Claudins, which comprise a 27-member protein family of tetra-transmembrane proteins, are the major structural and functional components of the TJ seal (Markov et al., 2015). The expression profile and TJ-sealing functions of the claudins differ among tissues. However, it has been reported that the BBB is more permeable to molecules with a molecular weight <800 Da in claudin (CLDN)-5-deficient mice than in wild-type mice (Nitta et al., 2003). In addition, knockdown of *Cldn-5* in mice leads to accumulation of small-molecular-weight molecules (562 Da) in the brain (Campbell et al., 2008). Together, these findings suggest that CLDN-5 is a potential target for targeted delivery of drugs to the CNS via

JPET Fast Forward. Published on August 17, 2017 as DOI: 10.1124/jpet.117.243014
This article has not been copyedited and formatted. The final version may differ from this version.

paracellular transport.

Here, we generated four anti-CLDN-5 monoclonal antibodies (mAbs) and examined the effects of these mAbs on the integrity of the TJ seal and the permeation of solutes in a model of the mammalian BBB.

Materials and methods

Animals

Male BXSB mice (6 weeks old), female BALB/c nu/nu mice (6 weeks old), and female Wistar rats (6 weeks old) were purchased from Shimizu Laboratory Supplies (Kyoto, Japan). All animals were maintained under controlled conditions of a 12:12-h light:dark cycle at 23 ± 1.5 ℃. The rodents were given *ad libitum* access to food and water. Animal experiments were approved by Osaka University (Osaka, Japan).

Cells

L cells stably expressing mouse CLDN-5 were kindly provided by Dr. S. Tsukita (Kyoto University, Kyoto, Japan). HT-1080 cells stably expressing human CLDN-1, -2, -3, -4, -5, -6, or -7 were developed as described previously (Hashimoto et al., 2016). P3U1 mouse myeloma cells, MDCKII cells, Phoenix-A packaging cells, and Caco-2 and T84 human intestinal cells were purchased from ATCC (Manassas, VA).

HT1080 cells (a cell line of human fibrosarcoma) are used for characterization of claudin binders because HT1080 cells are claudin-negative cells (Neesse et al., 2013; Mosley et al., 2015; Nakajima et al., 2015; Fukaswa et al., 2015). MDCKII cells (a cell line of canine epithelial cell) are a representative model for characterization of CLDN-5-based paracellular permeation and tight junction integrity (Amasheh et al., 2005; Del Vecchio et al., 2012; Piehl et al., 2010; Wen et al., 2004). HT-1080 cells and MDCKII cells expressing various claudins were prepared as described previously with minor modifications (Hashimoto et al., 2016). cDNAs encoding cynomolgus monkey CLDNs and four human CLDN-5/human CLDN-1 chimeric mutants were commercially

synthesized by Invitrogen (Carlsbad, CA) and inserted into pCX4pur vector (Akagi et al., 2000). The cDNAs encoding the four human CLDN-5/mouse CLDN-5 chimeric mutants were generated by means of site-directed mutagenesis of pCX4pur encoding human or mouse CLDN-5. The resulting vectors were transfected into Phoenix-A cells by using the X-tremeGENE HP DNA transfection reagent (Roche Diagnostics, Mannheim, Germany), and the retrovirus-containing supernatant was harvested 48 h after transfection. The retrovirus-containing supernatant was mixed with 8 μg/mL Polybrene (hexadimethrine bromide; Sigma-Aldrich, Melbourne, Australia) and used to transduce HT-1080 or MDCKII cells. Stably transduced cells were selected by using 5 μg/mL puromycin (InvivoGen, San Diego, CA).

L cells, HT-1080 cells, MDCKII cells, and Phoenix-A cells were maintained in Dulbecco's modified Eagle's medium (DMEM) supplemented with 10% heat-inactivated fetal bovine serum (FBS) (Nichirei Biosciences, Tokyo, Japan), 100 U/mL penicillin, and 100 μg/mL streptomycin (Nacalai Tesque, Kyoto, Japan). P3U1 cells were maintained in RPMI1640 medium supplemented with 10% heat-inactivated FBS, 100 U/mL penicillin, and 100 μg/mL streptomycin. All hybridomas were maintained in Hybridoma-SFM medium (Gibco, Grand Island, NY) supplemented with 10% BM Condimed H1 (Roche Diagnostics). Caco-2 cells were maintained in modified Eagle's medium supplemented with 10% FBS, 100 U/mL penicillin, and 100 μg/mL streptomycin. T84 cells were maintained in a 1:1 mixture of DMEM and Ham's F-12 supplemented with 10% FBS, 100 U/mL penicillin, and 100 μg/mL streptomycin. All cells were incubated at 37 °C under 5% CO_2.

Generation and purification of anti-CLDN-5 mAbs

Male BXSB mice and female Wistar rats were immunized every 2 weeks for 8 weeks with a eukaryotic expression vector encoding human CLDN-5, which is proprietary technology of GENOVAC GmbH (Freiburg, Germany). To generate hybridoma cells, lymphocytes were harvested 7 days after the final immunization and fused with P3U1 cells by using polyethylene glycol 1000 (Roche Diagnostics). Hybridoma cells producing antibody that reacted with human CLDN-5 were screened for the selectivity of their antibodies to bind to HT-1080/human CLDN-5 but not HT-1080/mock cells. The mAb subclass was determined by using a mouse or rat immunoglobulin isotyping enzyme-linked immunosorbent assay kit (BD Biosciences, Franklin Lakes, NJ).

Purified mAbs were prepared as described previously (Hashimoto et al., 2016). Briefly, hybridoma cells were inoculated intraperitoneally into pristane-injected female BALB/c nu/nu mice, resulting in the production of ascitic fluid containing the mAbs. The mAbs were purified from the ascitic fluid by using Protein G Sepharose 4 Fast Flow columns (GE Healthcare, Princeton, NJ). The purified mAbs were then dialyzed against phosphate-buffered saline (pH 7.4, PBS) and stored at −30 °C. The concentration of mAbs was quantified with a BCA protein assay kit using bovine serum albumin (BSA) as the standard (Pierce Chemical, Rockford, IL).

Preparation of C-CPE mutant

A mutant of the C-terminal half of a *Clostridium perfringens* enterotoxin ($C\text{-}CPE_{Y306W/S313H}$, C-CPEmt) that recognizes a broad range of claudins, including CLDN-5, was prepared as described previously with minor modifications (Takahashi et al., 2012; Protze et al., 2015). Briefly, *Escherichia coli* BL-21 (DE 3) was transformed with the pET16b vector encoding C-CPEmt, and protein expression was induced by the

addition of isopropyl-d-thiogalactopyranoside. The cells were then harvested and lysed in buffer A (10 mM Tris–HCl [pH 8.0], 400 mM NaCl, 5 mM $MgCl_2$, 0.1 mM phenylmethanesulfonyl fluoride, 1 mM 2-mercaptoethanol, and 10% glycerol). The 10× His-tagged C-CPEmt was isolated from the cell lysate by means of affinity chromatography with an immobilized metal affinity chromatography column (HisTrap HP column, GE Healthcare). The buffer was exchanged with PBS by gel filtration (PD-10, GE Healthcare) and stored at −80 °C. The concentration of C-CPEmt was quantified with a BCA protein assay kit.

Flow cytometric analysis

To analyze the binding specificity of the anti-CLDN-5 mAbs, cells expressing the various claudins were detached from the culture plates. The cells were then incubated with the supernatants of hybridomas or with purified mAbs (5 μg/mL) and then stained with fluorescence-conjugated goat anti-mouse or rat IgG (Jackson ImmunoResearch, West Grove, PA). A mixture of C-CPEmt and anti-His tag antibody (Sigma-Aldrich) was used as the positive control.

Western blotting

To examine the expression level of several TJ proteins in CLDN-5-expressing HT-1080 and MDCKII cells, Caco-2 cells, and T84 cells, cell lysates were subjected to SDS-polyacrylamide gel electrophoresis and then transferred to polyvinylidene difluoride membranes. After blocking with 5% skimmed milk containing T-TBS (Tris-buffered saline containing 0.05% Tween-20), the membranes were incubated with rabbit anti-ZO-1 (Invitrogen, cat. no. 40-2200), rabbit anti-occludin (Invitrogen,

71-1500), rabbit anti-CLDN-1 (Invitrogen, 51-9000), rabbit anti-CLDN-2 (Invitrogen, 51-6100), rabbit anti-CLDN-3 (Invitrogen, 34-1700), mouse anti-CLDN-4 (Invitrogen, 32-9400), or rabbit anti-CLDN-5 (Sigma-Aldrich, SAB4502981) in 2% skimmed milk containing T-TBS for 12 h at 4 °C. Mouse anti-β-actin (Sigma-Aldrich, AC-15) was used as the loading control.

After incubation of the primary antibodies, the membranes were incubated with a horseradish peroxidase–conjugated anti-mouse or anti-rabbit antibody (Jackson ImmunoResearch) in T-TBS and then incubated for 2 h at room temperature. After washing with T-TBS, the membranes were treated with Chemi-Lumi Super (Nacalai Tesque) to detect the horseradish peroxidase, and chemiluminescent signals were imaged with an LAS4100 imager (GE Healthcare, Princeton, NJ).

Measurement of the electrical resistance of cell monolayers

Trans-epithelial/endothelial electrical resistance (TEER), which reflects the integrity of the TJ seal, was measured by using a Millicell ERS Ohmmeter (Millipore, Eschborn, Germany) and a culture plate warmer.

To measure the TEER of monolayers of CLDN-5-expressing MDCKII cells, 0.8×10^5 cells of mock MDCKII cells or MDCKII cells expressing human, cynomolgus monkey, or mouse CLDN-5 were seeded onto Falcon cell culture inserts (polyester membrane, 0.4 μm pore size, 0.3 cm^2 culture area, BD Bioscience) and cultured for one week (upper compartment 0.3 mL, lower compartment 0.9 mL). After exchange of 90 μL of medium from the lower compartment with 90 μL of 300 or 900 μg/mL of mAb in PBS (final concentration, 30 or 90 μg/mL, respectively), the TEER of the monolayer was measured for 12 h. Treatments with PBS (vehicle), mouse IgG, or rat IgG were

used as negative controls, and treatment of the lower compartment with 60 μg/mL of C-CPEmt was used as the positive control.

To measure the TEER of a monolayer of cynomolgus monkey brain microvasculature cells, a triple co-culture model (PharmaCo-cell, Nagasaki, Japan) was cultured for 5 days (Nakagawa et al., 2009). After exchange of 30 μL of medium from the upper compartment with 30 μL of 500 or 1500 μg/mL of mAb in PBS (final concentration, 50 or 150 μg/mL, respectively), the TEER of the monolayer was measured for 12 h. Treatment of the upper compartment with 100 μg/mL of C-CPEmt in was used as the positive control for TEER alteration.

To measure the TEER of a monolayer of Caco-2 or T84 human intestinal cells, cells (0.8×10^5 cells) were seeded into Falcon cell culture inserts and cultured for 10 days. After exchange of 30 and 90 μL medium from the upper and lower compartment with 30 and 90 μL of 1500 μg/mL of mAb in PBS, respectively (final concentration, 150 μg/mL), the TEER of the monolayers was measured for 12 h. Treatments with PBS (vehicle), mouse IgG, and rat IgG were used as negative controls, and treatment with 100 μg/mL of C-CPEmt in both compartments was used as the positive control.

Measurement of the permeation of solutes through cell monolayers

After measurement of the TEER of monolayers of cynomolgus monkey brain microvasculature cells, the permeability of the monolayers to sodium fluorescein (FNa; 376 Da; Wako Pure Chemical, Osaka, Japan) or fluorescein isothiocyanate-labeled dextran with an average molecular weight of 4 kDa (FD-4, Sigma-Aldrich) was determined. After washes with DMEM (without FBS), cell culture inserts were transferred to 24-well plates (Grainer, Frickenhausen, Germany) containing 0.9 mL of

JPET Fast Forward. Published on August 17, 2017 as DOI: 10.1124/jpet.117.243014
This article has not been copyedited and formatted. The final version may differ from this version.

DMEM (without FBS). The medium in the upper chamber was then changed to 0.2 mL of 10 μg/mL FNa or 1 mg/mL FD-4 in DMEM (without FBS), and the culture inserts were incubated for 30 min on a plate warmer. Samples were collected from the lower compartment, and the concentration of tracer was measured by using a TriStar LB 941 plate reader (Berthold Technologies, Bad Wildbad, Germany). Apparent permeability coefficients (P_{app}) (cm/s) were calculated by using the following equation:

$$P_{app} = \frac{\text{volume of lower compartment} \times \text{initial tracer concentration}}{\text{assay time} \times \text{surface area of the culture inserts} \times \text{concentration of tracer in the sample}}$$

Statistical analysis

Data were analyzed by using One-way ANOVA followed by Bonferroni's post hoc test. Statistical significance for all comparisons was set at $P < 0.05$.

Results

Generation and characterization of mAbs targeting the extracellular loop domains of human CLDN-5

Previously, we generated anti-CLDN-1 and anti-CLDN-4 mAbs by using DNA immunization methods (Fukasawa et al., 2015; Hashimoto et al., 2016). In the present study, we used these techniques to generate anti-CLDN-5 mAbs by immunizing BXSB mice and Wistar rats with a plasmid encoding human CLDN-5. Four mAbs targeting the extracellular loop domains (ECLs) of human CLDN-5 were isolated: M11 and M48 from the mice and R2 and R9 from the rats (Figure 1A). All four mAbs specifically bound to CLDN-5 but not to CLDN-1 to -4, -6, or -7 (Figure 1B). A cross-species reactivity analysis of the mAbs revealed that all four mAbs bound to human and cynomolgus monkey CLDN-5, but not to mouse CLDN-5, except for R9, which also weakly bound to mouse CLDN-5 (Figure 1C).

We next investigated the epitopes of CLDN-5 recognized by the anti-CLDN-5 mAbs by swapping amino acids 26–78 in ECL1 and amino acids 147–162 in ECL2 of human CLDN-5 with the corresponding amino acids in human CLDN-1 (chimeric mutants 1-5, and 5-1, respectively; Figure 2A). C-CPEmt, which is a broad-specific binder of CLDN-1 to -7, bound to these mutants (Figure 2B), indicating that these chimeric mutants had normal tropism as transmembrane proteins and were correctly recruited to the cell membrane. However, substitution of ECL1 of human CLDN-5 with that of human CLDN-1 (chimeric mutant 1-5) attenuated the binding of M11 and R2, but not that of M48 or R9 (Figure 2B), and substitution of ECL2 of human CLDN-5 with that of human CLDN-1 (chimeric mutant 5-1) attenuated the binding of M48 and R9, but not

JPET Fast Forward. Published on August 17, 2017 as DOI: 10.1124/jpet.117.243014
This article has not been copyedited and formatted. The final version may differ from this version.

that of M11 or R2 (Figure 2B). These findings suggested that the epitope for M11 and R2 was contained in ECL1, whereas that for M48 and R9 was contained in ECL2. Alignment of the amino acid sequences of human, cynomolgus monkey, and mouse CLDN-5 revealed three candidate epitopes (Figure 2C): aspartic acid (D) at position 68 in ECL1, threonine (T) at position at 75 in ECL1, and serine (S) at position 151 in ECL2. Therefore, we next generated transfectants stably expressing mutant human CLDN-5 containing the substitutions D68E, T75A, and S151T (Figure 2D). The D68E substitution attenuated the binding of M11 and R2, and the S151T substitution partly attenuated the binding of M48 and R9 (Figure 2E). These results suggest that in human CLDN-5, the dominant epitope of M11 and R2 is D68 in ECL1 and that of M48 and R9 is S151 in ECL2.

Effects of the anti-CLDN-5 mAbs on TJ integrity in MDCKII transfectants

Next, to investigate whether the anti-CLDN-5 mAbs decreased TJ integrity in a CLDN-5-dependent manner, MDCKII transfectants expressing human (h), cynomolgus monkey (c), or mouse (m) CLDN-5 were established (Figure 3A). TJ integrity, as determined by TEER, peaked at 20–30, 230–250, 250–270, and 400–420 $\Omega \cdot cm^2$ in MDCKII/mock, MDCKII/hCLDN-5, MDCKII/cCLDN-5, and MDCKII/mCLDN-5 cells, respectively (Supplementary figure 1). Treatment of all transfectants with C-CPEmt decreased TJ integrity (Figure 3B). All four of the anti-CLDN-5 mAbs dose- and time-dependently decreased TEER in the hCLDN-5- and cCLDN-5-expressing transfectants. In contrast, none of the anti-CLDN-5 mAbs affected TJ integrity in the mCLDN-5-expressing transfectant (Figure 3B). These findings suggest that M11, M48, R2, and R9 decreased TJ integrity by interacting with CLDN-5. TEER values returned

JPET Fast Forward. Published on August 17, 2017 as DOI: 10.1124/jpet.117.243014
This article has not been copyedited and formatted. The final version may differ from this version.

to baseline 24 h after the anti-CLDN-5 mAbs were removed (Supplementary figure 2). The binding affinity of R9 to mouse CLDN-5 may not have been strong enough to decrease TJ integrity in the mouse CLDN-5 transfectant (Supplementary figure 3).

Next, we investigated the effects of the anti-CLDN-5 mAbs on the BBB by using a commercially available BBB model composed of a co-culture of cynomolgus monkey brain microvasculature endothelial cells, rat pericytes, and rat astrocytes (Nakagawa et al., 2009). Treatment of the model BBB with the anti-CLDN-5 mAbs dose- and time-dependently reduced TEER (Figure 4A). In addition, no cytotoxicity was observed after treatment with the anti-CLDN-5 mAbs (Supplementary figure 4). M48 and R9 modulated TJ integrity more than did M11 and R2, suggesting that binders targeting ECL2 of CLDN-5 may modulate TJ integrity more than binders targeting ECL1.

Next, we clarified whether the anti-CLDN-5 mAbs increased the permeability of the model BBB to solutes by using a fluorescein dye with a molecular mass of 376 Da and fluorescein isothiocyanate-labeled dextran with an average molecular mass of 4 kDa (FD-4). Control IgG did not increase the permeability of the model BBB to the fluorescein dye or FD-4 (Figures 4B and 4C). However, treatment with the anti-CLDN-5 mAbs significantly and dose-dependently increased the permeability of the model BBB to the fluorescein dye and FD-4 compared with vehicle ($p < 0.05$; Figures 4B and 4C). R9 was the most potent permeation enhancer: P_{app} of fluorescein dye: vehicle, 3.8×10^{-6} cm/s vs. R9 (150 μg/mL) 12.3×10^{-6} cm/s; P_{app} of FD-4: vehicle, 1.0×10^{-6} cm/s vs. R9 (150 μg/mL) 6.0×10^{-6} cm/s (Figures 4B and 4C).

To examine the cell specificity of the TJ-integrity modulating activity of the anti-CLDN-5 mAbs, we investigated the effect of the anti-CLDN-5 mAbs on TJ integrity in two human intestinal epithelium models: Caco-2 and T84 cells. Immunoblot

analyses showed that both Caco-2 and T84 cells expressed CLDN-5, but the expression of CLDN-5 in the Caco-2 cells was much lower than that in the T84 cells (Figure 5A). Although C-CPEmt decreased the TEER in monolayers of both Caco-2 and T84 cells, the anti-CLDN-5 mAbs did not even at 150 μg/mL (Figure 5B), suggesting that anti-CLDN-5 mAbs might be BBB-specific modulators.

Discussion

Although the concept of CLDN-5-targeted drug delivery to the brain was proposed more than a decade ago (Nitta et al., 2003), the concept remains unproven because no CLDN-5-specific binders have been developed. Here, we used DNA immunization to generate CLDN-5-specifc mAbs that targeted the extracellular domains of CLDN-5, and we found that these mAbs time- and dose-dependently decreased TJ integrity and increased the permeation of solutes across a model BBB.

CLDN-5 is ubiquitously expressed in the mammalian body, and CLDN-5 deficient mice die within 10 h after birth (Morita et al., 1999; Nitta et al., 2003). This suggests that treatment with CLDN-5 binders may induce severe side effects. However, the expression level of CLDN-5 in peripheral organs and peripheral microvascular endothelial cells is lower than that in brain microvasculature cells (Morita et al., 1999; Rahner et al., 2001). In addition, in the peripheral organs, other claudins are also likely involved in maintenance of TJ integrity and organ homeostasis (Tamura and Tsukita, 2014), and the TJs between peripheral microvascular endothelial cells are not well developed compared with those in the BBB (Morita et al., 1999). This may explain why knockdown of *Cldn-5* in mice increases permeation of solutes to the brain without any apparent adverse effects (Campbell et al., 2008; Keaney et al., 2015). Indeed, in brain-injured mice, knockdown of CLDN-5 mRNA expression by using short interfering RNA leads to improved cognitive outcomes without significant histological abnormalities in the major organs (Campbell et al., 2012). Consistent with this, we found in the present study that treatment with anti-CLDN-5 mAbs did not result in cytotoxicity *in vitro* or toxicity. Taken together, these findings suggest that CLDN-5 is a

promising target for the development of drug delivery systems targeting the CNS.

Claudins form TJ strands via cis-interactions between ECLs in the same cell membrane, and adjacent TJ strands interact via trans-interactions between ECLs of adjacent cells, leading to sealing of the paracellular space (Zihni et al., 2016). The crystal structure of CLDN-15 revealed that the cis- and trans-interactions among ECLs may determine the permeability of TJs (Suzuki et al., 2014; Suzuki et al., 2015). We previously found that a CLDN-3/-4 binder (C-CPE) enhanced the permeation of solutes across the mucosal membrane, indicating that CLDN binders may enhance permeation via the paracellular pathway by modulating the TJ seal (Kondoh et al., 2005; Uchida et al., 2010). Cysteine 54, cysteine 64, leucine 50, and tryptophan 51 in ECL1 of CLDN-5 are involved in paracellular barrier formation (Wen et al., 2004). Phenylalanine 147, tyrosine 148, glutamine 156, tyrosine 158, and glutamic acid 159 in ECL2 of CLDN-5 are involved in the trans-interactions between cells (Piontek et al., 2008). In the present study, we found that C-CPEmt, M11, M48, R2, and R9 decreased TJ integrity in a model of the BBB. C-CPEmt mainly binds to CLDN-5 at aspartic acid 149/threonine 151 (Protze et al., 2015), M48 and R9 interacted with ECL2 of CLDN-5, and M11 and R2 interacted with ECL1 of CLDN-5. These findings indicate that binders targeting ECL1 and ECL2 of CLDN-5 may prevent the cis- and trans-interactions of CLDN-5 in the TJ seal, resulting in enhancing permeation of molecules across the BBB.

Treatment of cynomolgus monkey brain endothelial cells with anti-CLDN-5 mAbs altered the localization of CLDN-5 from the borders between cells to the cytosol (Supplementary figure 5). This finding is consistent with previous reports that a CLDN-4 binder decreased the amount of CLDN-4 in TJs and a CDLN-1 and -5 binder increased the intracellular localization of CLDN-1 and -5 (Staat et al., 2015). Together,

these findings suggest that the binding of mAbs to the ECLs of CLDN-5 may induce intracellular uptake of the binder-bound CLDN-5, thereby disrupting the CLDN-5 trans-interactions in the TJ seal between adjacent cells and loosening the seal in the paracellular space.

The currently available drug delivery systems targeting the CNS, injection of mannitol and treatment with pulsed sound, disrupt the TJ seal and open the paracellular space to 200 nm and 50 nm, respectively, leading to the diffusion of substances, such as albumin, into the brain (Rapoport, 2000; Chen and Konofagou, 2014; Kovacs et al., 2017). Claudins in TJs form charge-selective pores with a diameter of 4 nm, and therefore have unique roles in the size- and charge-selective paracellular transport of solutes across the membrane (Furuse and Tsukita, 2006; Van Itallie and Anderson, 2013). In addition, the claudin-based strands within TJs are dynamic structures that undergo continuous local annealing and breaking (Sasaki et al., 2003). Therefore, the pore-forming and dynamic movements of the TJ seal are determined by the specific combination of claudins in the strands, which differs depending on the tissue (Gunzel and Fromm, 2012; Van Itallie and Anderson, 2013). C-CPEmt, a broad-specific CLDN binder to CLDN-1~-7, decreased integrity of TJ seal in BBB models and intestinal models. In contrast, anti-CLDN-5 mAbs reduced integrity of TJ seal in only BBB models. These findings strongly indicate that inhibition of claudins modulates or controls the paracellular transport of drugs in a size- and charge-dependent manner. Mice in which the expression of CLDN-5 is silenced also allow increased passage of molecules with molecular weights up to 562 Da across the BBB while retaining normal TJ morphology in the BBB (Campbell et al., 2008). Removal of CLDN-5 was left to TJs containing CLDN-12 (Nitta et al. 2003). It is likely that CLDN-5 binders will provide

JPET Fast Forward. Published on August 17, 2017 as DOI: 10.1124/jpet.117.243014
This article has not been copyedited and formatted. The final version may differ from this version.

new options for the development of novel drug delivery systems targeting the CNS that are based on modulation, rather than disruption, of the TJ seal.

In conclusion, the anti-CLDN-5 mAbs developed here are the first CLDN-5-specific binders. The present results suggest that CLDN-5 binders are a potential lead for the development of novel drug delivery systems targeting the CNS.

JPET Fast Forward. Published on August 17, 2017 as DOI: 10.1124/jpet.117.243014
This article has not been copyedited and formatted. The final version may differ from this version.

Acknowledgements

We thank all of the members of our laboratory for their useful comments. We also thank Mrs. Yuko Fujieda for her excellent technical assistance.

Author Contributions

Participated in research design: Y.H., K.S., Y.O., H.T., K.E., T.S. and M.K.

Conducted experiments: Y.H., K.S., K.E., M.T., H.T. and Y.S.

Contributed new reagents or analytic tools: Y.O., H.T., and A.W.

Performed data analysis: Y.H., K.S., Y.O., T.D., K.Y. and M.K.

Wrote or contributed to the writing of the manuscript: Y.H., Y.O., H.T., T.S., T.D., K.Y. and M.K.

References

Akagi T, Shishido T, Murata K and Hanafusa H (2000) v-Crk activates the phosphoinositide 3-kinase/AKT pathway in transformation. *Proc Natl Acad Sci U S A* **97**: 7290-7295.

Amasheh S, Schmidt T, Mahn M, Florian P, Mankertz J, Tavalali S, Gitter AH, Schulzke JD, Fromm M (2005) Contribution of claudin-5 to barrier properties in tight junctions of epithelial cells. *Cell Tissue Res* **321**: 89-96.

Betz AL, Firth JA and Goldstein GW (1980) Polarity of the Blood-Brain-Barrier - Distribution of Enzymes between the Luminal and Antiluminal Membranes of Brain Capillary Endothelial-Cells. *Brain Res* **192**: 17-28.

Campbell M, Hanrahan F, Gobbo OL, Kelly ME, Kiang AS, Humphries MM, Nguyen ATH, Ozaki E, Keaney J, Blau CW, Kerskens CM, Cahalan SD, Callanan JJ, Wallace E, Grant GA, Doherty CP and Humphries P (2012) Targeted suppression of claudin-5 decreases cerebral oedema and improves cognitive outcome following traumatic brain injury. *Nat Commun* **3**: 849.

Campbell M, Kiang AS, Kenna PF, Kerskens C, Blau C, O'Dwyer L, Tivnan A, Kelly JA, Brankin B, Farrar GJ and Humphries P (2008) RNAi-mediated reversible opening of the blood-brain barrier. *J Gene Med* **10**: 930-947.

Carpentier A, Canney M, Vignot A, Reina V, Beccaria K, Horodyckid C, Karachi C, Leclercq D, Lafon C, Chapelon JY, Capelle L, Cornu P, Sanson M, Hoang-Xuan K, Delattre JY and Idbaih A (2016) Clinical trial of blood-brain barrier disruption by pulsed ultrasound. *Sci Transl Med* **8**: 343re342.

Chen H and Konofagou EE (2014) The size of blood-brain barrier opening induced by

focused ultrasound is dictated by the acoustic pressure. *J Cereb Blood Flow Metab* **34**: 1197-204

Del Vecchio G, Tscheik C, Tenz K, Helms HC, Winkler L, Blasig R and Blasig IE (2012) Sodium caprate transiently opens claudin-5-containing barriers at tight junctions of epithelial and endothelial cells. *Mol Pharm* **9**: 2523-2533.

Fukasawa M, Nagase S, Shirasago Y, Iida M, Yamashita M, Endo K, Yagi K, Suzuki T, Wakita T, Hanada K, Kuniyasu H and Kondoh M (2015) Monoclonal antibodies against extracellular domains of claudin-1 block hepatitis C virus infection in a mouse model. *J Virol* **89**: 4866-4879.

Furuse M (2014) Molecular Organization of Tricellular Tight Junctions. *Yakugaku Zasshi* **134**: 615-621.

Furuse M and Tsukita S (2006) Claudins in occluding junctions of humans and flies. *Trends Cell Biol* **16**: 181-188.

Gribkoff VK and Kaczmarek LK The need for new approaches in CNS drug discovery: Why drugs have failed, and what can be done to improve outcomes. *Neuropharmacology*:in press.

Gunzel D and Fromm M (2012) Claudins and other tight junction proteins. *Compr Physiol* **2**: 1819-1852.

Hashimoto Y, Kawahigashi Y, Hata T, Li X, Watari A, Tada M, Ishii-Watabe A, Okada Y, Doi T, Fukasawa M, Kuniyasu H, Yagi K and Kondoh M (2016) Efficacy and safety evaluation of claudin-4-targeted antitumor therapy using a human and mouse cross-reactive monoclonal antibody. *Pharmacol Res Perspect* **4**: e00266.

Heidenreich M and Zhang F (2016) Applications of CRISPR-Cas systems in neuroscience. *Nat Rev Neurosci* **17**: 36-44.

Kaitlin KI (2014) CNS drugs have lower regulatory success rate, take longer to develop. *Tufts CSDD Impact Reports* **16**: 1-4.

Keaney J, Walsh DM, O'Malley T, Hudson N, Crosbie DE, Loftus T, Sheehan F, McDaid J, Humphries MM, Callanan JJ, Brett FM, Farrell MA, Humphries P and Campbell M (2015) Autoregulated paracellular clearance of amyloid-beta across the blood-brain barrier. *Sci Adv* **1**: e1500472.

Kondoh M, Masuyama A, Takahashi A, Asano N, Mizuguchi H, Koizumi N, Fujii M, Hayakawa T, Horiguchi Y and Watanbe Y (2005) A novel strategy for the enhancement of drug absorption using a claudin modulator. *Mol Pharmacol* **67**: 749-756.

Kovacs ZI, Kim S, Jikaria N, Qureshi F, Milo B, Lewis BK, Bresler M, Burks SR, Frank JA (2017) Disrupting the blood-brain barrier by focused ultrasound induces sterile inflammation. *Proc Natl Acad Sci USA* **114**: E75-E84.

Laksitorini M, Prasasty VD, Kiptoo PK and Siahaan TJ (2014) Pathways and progress in improving drug delivery through the intestinal mucosa and blood-brain barriers. *Ther Deliv* **5**: 1143-1163.

Lipinski CA, Lombardo F, Dominy BW and Feeney PJ (2001) Experimental and computational approaches to estimate solubility and permeability in drug discovery and development settings. *Adv Drug Deliver Rev* **46**: 3-26.

Liu Y and Deng WB (2016) Reverse engineering human neurodegenerative disease using pluripotent stem cell technology. *Brain Res* **1638**: 30-41.

Markov AG, Aschenbach JR and Amasheh S (2015) Claudin clusters as determinants of epithelial barrier function. *IUBMB Life* **67**: 29-35.

Morita K, Sasaki H, Furuse M and Tsukita S (1999) Endothelial claudin:

claudin-5/TMVCF constitutes tight junction strands in endothelial cells. *J Cell Biol* **147**: 185-194.

Mosley M, Knight J, Neesse A, Michl P, Iezzi M, Kersemans V and Cornelissen B (2015) Claudin-4 SPECT Imaging Allows Detection of Aplastic Lesions in a Mouse Model of Breast Cancer. *J Nucl Med* **56**:745-751.

Nakagawa S, Deli MA, Kawaguchi H, Shimizudani T, Shimono T, Kittel A, Tanaka K and Niwa M (2009) A new blood-brain barrier model using primary rat brain endothelial cells, pericytes and astrocytes. *Neurochem Int* **54**: 253-263.

Nakajima M, Nagase S, Iida M, Takeda S, Yamashita M, Watari A, Shirasago Y, Fukasawa M, Takeda H, Sawasaki T, Yagi K, Kondoh M (2015) Claudin-1 Binder Enhances Epidermal Permeability in a Human Keratinocyte Model. *J Pharmacol Exp Ther* **354**:440-447.

Neesse A, Hahnenkamp A, Griesmann H, Buchholz M, Hahn SA, Maghnouj A, Fendrich V, Ring J, Sipos B, Tuveson DA, Bremer C, Gress TM, Michl P (2013) Claudin-4-targeted optical imaging detects pancreatic cancer and its precursor lesions. *Gut* **62**:1034-1043.

Nitta T, Hata M, Gotoh S, Seo Y, Sasaki H, Hashimoto N, Furuse M and Tsukita S (2003) Size-selective loosening of the blood-brain barrier in claudin-5-deficient mice. *J Cell Biol* **161**: 653-660.

Pardridge WM (2005) The blood-brain barrier: bottleneck in brain drug development. *NeuroRx* **2**: 3-14.

Pardridge WM (2007) Drug targeting to the brain. *Pharm Res* **24**: 1733-1744.

Pardridge WM and Boado RJ (2012) Reengineering biopharmaceuticals for targeted delivery across the blood-brain barrier. *Methods Enzymol* **503**: 269-292.

Piehl C, Piontek J, Cording J, Wolburg H and Blasig IE (2010) Participation of the second extracellular loop of claudin-5 in paracellular tightening against ions, small and large molecules. *Cell Mol Life Sci* **67**: 2131-2140.

Piontek J, Winkler L, Wolburg H, Muller SL, Zuleger N, Piehl C, Wiesner B, Krause G and Blasig IE (2008) Formation of tight junction: determinants of homophilic interaction between classic claudins. *FASEB J* **22**: 146-158.

Protze J, Eichner M, Piontek A, Dinter S, Rossa J, Blecharz KGZ, Vajkoczy P, Piontek J and Krause G (2015) Directed structural modification of *Clostridium perfringens* enterotoxin to enhance binding to claudin-5. *Cell Mol Life Sci* **72**: 1417-1432.

Rahner C, Mitic LL and Anderson JM (2001) Heterogeneity in expression and subcellular localization of claudins 2, 3, 4, and 5 in the rat liver, pancreas, and gut. *Gastroenterology* **120**: 411-422.

Rapoport SI (2000) Osmotic opening of the blood-brain barrier: principles, mechanism, and therapeutic applications. *Cell Mol Neurobiol* **20**: 217-230.

Rubin LL and Staddon JM (1999) The cell biology of the blood-brain barrier. *Annu Rev Neurosci* **22**: 11-28.

Sasaki H, Matsui C, Furuse K, Mimori-Kiyosue Y, Furuse M, Tsukita S (2003) Dynamic behavior of paired claudin strands within apposing plasma membranes. *Proc Natl Acad Sci USA* **100**: 3971-3976.

Staat C, Coisne C, Dabrowski S, Stamatovic SM, Andjelkovic AV, Wolburg H, Engelhardt B and Blasig IE (2015) Mode of action of claudin peptidomimetics in the transient opening of cellular tight junction barriers. *Biomaterials* **54**: 9-20.

Suzuki H, Nishizawa T, Tani K, Yamazaki Y, Tamura A, Ishitani R, Dohmae N, Tsukita

S, Nureki O and Fujiyoshi Y (2014) Crystal structure of a claudin provides insight into the architecture of tight junctions. *Science* **344**: 304-307.

Suzuki H, Tani K, Tamura A, Tsukita S and Fujiyoshi Y (2015) Model for the Architecture of Claudin-Based Paracellular Ion Channels through Tight Junctions. *J Mol Biol* **427**: 291-297.

Takahashi A, Saito Y, Kondoh M, Matsushita K, Krug SM, Suzuki H, Tsujino H, Li XR, Aoyama H, Matsuhisa K, Uno T, Fromm M, Hamakubo T and Yagi K (2012) Creation and biochemical analysis of a broad-specific claudin binder. *Biomaterials* **33**: 3464-3474.

Tamura A and Tsukita S (2014) Paracellular barrier and channel functions of TJ claudins in organizing biological systems: Advances in the field of barriology revealed in knockout mice. *Semin Cell Dev Biol* **36**: 177-185.

Uchida H, Kondoh M, Hanada T, Takahashi A, Hamakubo T and Yagi K (2010) A claudin-4 modulator enhances the mucosal absorption of a biologically active peptide. *Biochem Pharmacol* **79**: 1437-1444.

Van Itallie CM and Anderson JM (2013) Claudin interactions in and out of the tight junction. *Tissue Barriers* **1**: e25247.

Wen HJ, Watry DD, Marcondes MCG and Fox HS (2004) Selective decrease in paracellular conductance of tight junctions: role of the first extracellular domain of claudin-5. *Mol Cell Biol* **24**: 8408-8417.

Zihni C, Mills C, Matter K and Balda MS (2016) Tight junctions: from simple barriers to multifunctional molecular gates. *Nat Rev Mol Cell Bio* **17**: 564-580.

Footnotes

Financial support: This work was supported by a Health and Labour Sciences Research Grant from the Ministry of Health, Labour and Welfare of Japan; a research grant from the Japan Agency for Medical Research and Development; a Grant-in-Aid for Scientific Research from the Ministry of Education, Culture, Sports, Science and Technology of Japan [grant number 24390042]; and funds from the Adaptable and Seamless Technology Transfer Program through Target-driven R&D Agency; Platform for Drug Discovery, Informatics, and Structural Life Science of the Ministry of Education, Culture, Sports, Science and Technology of Japan; and the Takeda Science Foundation. Y.H. was supported by a Research Fellowship for Young Scientists from the Japan Society for the Promotion of Science [grant number 15J10065].

Figure legends

Figure 1. Generation and characterization of monoclonal antibodies (mAbs) targeting human claudin (CLDN)-5.

A) Flow cytometric analysis. Mock-transfected or human CLDN-5–expressing HT-1080 cells were treated with the four generated mAbs (M11, M48, R2, or R9). The cells were then treated with fluorescein-labeled secondary antibodies, and mAb-bound cells were detected by flow cytometry. B) Claudin specificity of the mAbs. Mock-transfected or human CLDN–expressing HT-1080 cells were treated with the indicated mAbs or the C-terminal half of *Clostridium perfringens* enterotoxin (C-CPEmt). The cells were then treated with fluorescein-labeled secondary antibodies or anti-His-tag mAbs followed by fluorescein-labeled antibodies. mAb- or C-CPEmt-bound cells were detected by flow cytometry. C-CPEmt binding was used as the positive control. C) Species specificity of the mAbs. Human, cynomolgus monkey, or mouse CLDN-5–expressing HT-1080 cells were treated with the mAbs. The cells were then treated with fluorescein-labeled secondary antibodies, and mAb-bound cells were detected by flow cytometry.

Figure 2. Epitope mapping of the generated anti-claudin (CLDN)-5 antibodies.

A) Schematic illustration of the human CLDN-5/-1 chimeric constructs. Green represents the cell membrane. Amino acids 26–78 and 147–162 of the extracellular loop domains of human CLDN-5 were swapped with the corresponding amino acids of human CLDN-1 to generate the 1-5 and 5-1 mutant, respectively. B) Binding of the anti-CLDN-5 monoclonal antibodies (mAbs) to human CLDN-5/-1 chimeric mutants. Chimeric mutant–expressing HT1080 cells were treated with the anti-CLDN-5 mAbs or

C-terminal half of *Clostridium perfringens* enterotoxin (C-CPEmt), followed by incubation with fluorescein-labeled antibodies or anti-His-tag mAbs and fluorescein-labeled antibodies, respectively. mAb- or C-CPEmt-bound cells were detected by flow cytometry. C-CPEmt was used as the positive control for the chimeric mutants. C) Alignment of the amino acid sequences of human, cynomolgus monkey, and mouse CLDN-5. The sequences were obtained from the National Center for Biotechnology Information database (accession numbers: human, AAH19290.2; cynomolgus monkey, XP_005596069.1; and mouse, NP_038833.2). Gray highlights indicate putative transmembrane domains, predicted by the SOSUI program (http://harrier.nagahama-i-bio.ac.jp/sosui/). The amino acids at positions 68, 75, and 151 are enclosed within dashed lines. D) Schematic illustration of the human/mouse CLDN-5 mutants. Human CLDN-5/mouse CLDN-5 chimeric CLDNs were generated by single amino acid substitution in the extracellular loop domains of human CLDN-5 with the corresponding amino acids in mouse CLDN-5 (mutants D68E, T75A, and S151T). E) Binding of the anti-CLDN-5 mAbs to the human/mouse CLDN-5 chimeric mutants. Chimeric mutant–expressing HT1080 cells were treated with the anti-CLDN-5 mAbs or C-CPEmt, followed by incubation with fluorescein-labeled antibodies or anti-His-tag mAbs and fluorescein-labeled mAbs, respectively. The mAb- or C-CPEmt-bound cells were detected by flow cytometry. C-CPEmt was used as the positive control for the chimeric mutants.

Figure 3. Effect of the anti-claudin (CLDN)-5 mAbs on tight junction integrity in MDCKII transfectants.

A) Immunoblot analysis of TJ protein expression in MDCKII transfectants expressing

human (h), mouse (m), or cynomolgus monkey (c) CLDN-5. Cell lysates were subjected to SDS-polyacrylamide gel electrophoresis followed by immunoblotting onto a polyvinylidene fluoride membrane. The membranes were incubated with primary antibodies and secondary peroxidase-labeled antibodies. The reacted bands were detected with a chemiluminescence agent. B) Effects of anti-CLDN-5 mAbs on TEER in MDCKII cells stably expressing CLDN-5. Monolayers of the MDCKII transfectants were treated with PBS (vehicle), mouse IgG, rat IgG, anti-CLDN-5 mAbs, or C-CPEmt at the indicated concentrations for 12 h. Trans-epithelial/endothelial electrical resistance (TEER) was then monitored during the treatment. Data are presented as percent TEER relative to the value at 0 h. Data are representative of three independent experiments. Data are presented as mean ± SD (n = 3).

Figure 4. Effect of the anti-claudin (CLDN)-5 mAbs on an *in vitro* model of the blood–brain barrier.

A) Effects of anti-CLDN-5 mAbs on trans-epithelial/endothelial electrical resistance (TEER) in a BBB model. Monolayers of cynomolgus monkey brain microvasculature endothelial cells were apically treated with phosphate-buffered saline (vehicle), mouse IgG, rat IgG, anti-CLDN-5 mAbs, or C-CPEmt at the indicated concentrations for 12 h. TEER was monitored during the treatment. Data are expressed as percent TEER relative to the value at 0 h. Data are representative of three independent experiments. Data are presented as mean ± SD (n = 3). B, C) Effects of the anti-CLDN-5 mAbs on permeation of solutes. Cynomolgus monkey brain microvasculature endothelial cells were treated with anti-CLDN-5 mAbs or C-CPEmt at the indicated concentrations for 12 h. The cells were then incubated on the apical side with a fluorescein dye with a molecular mass of

376 Da (B) or with fluorescence-conjugated dextran with an average molecular mass of 4 kDa (C), and the apparent permeation of solutes (P_{app}) from the apical side to the basal side was measured. Data are representative of three independent experiments. Data are presented as mean ± SD (n = 3). *, $P < 0.05$ versus vehicle treatment.

Figure 5. Effect of anti-claudin (CLDN)-5 monoclonal antibodies (mAbs) on tight junction integrity in human intestinal cell monolayers.

A) Immunoblot analysis of tight junction proteins in Caco-2 and T84 cells. Cell lysates were subjected to SDS-polyacrylamide gel electrophoresis followed by immunoblot onto polyvinylidene fluoride membrane. The membranes were incubated with primary antibodies and secondary peroxidase-labeled antibodies. The reacted bands were detected with a chemiluminescence agent. B) Effects of the anti-CLDN-5 mAbs on trans-epithelial/endothelial electrical resistance (TEER) in Caco-2 and T84 monolayers. Monolayers of Caco-2 cells and T84 cells were treated with phosphate-buffered saline (vehicle), anti-CLDN-5 mAbs, mouse IgG, rat IgG, M11, or C-terminal half of *Clostridium perfringens* enterotoxin (C-CPEmt) at the indicated concentrations for 12 h. TEER was monitored during the treatment. Data are expressed as percent TEER relative to the value at 0 h. Data are representative of three independent experiments. Data are presented as mean ± SD (n = 3).

JPET Fast Forward. Published on August 17, 2017 as DOI: 10.1124/jpet.117.243014
This article has not been copyedited and formatted. The final version may differ from this version.

Table 1 Summary of epitope mapping

		Human CLDN-5/CLDN-1 chimera mutant		Human/mouse chimera CLDN-5 mutant		
Clone	Subclass	1-5	5-1	D68E	T75A	S151T
M11	Mouse IgG2b	−	+++	−	+++	+++
M48	Mouse IgG3	+++	−	+++	+++	−
R2	Rat IgG2a	−	+++	−	+++	+++
R9	Rat IgG2b	+++	−	+++	+++	+

+++, +, and − indicate strong, weak, and negligible binding reactivity of anti-CLDN-5 antibody against each chimera claudin (CLDN).

JPET Fast Forward. Published on August 17, 2017 as DOI: 10.1124/jpet.117.243014
This article has not been copyedited and formatted. The final version may differ from this version.

Figure 1.

A.

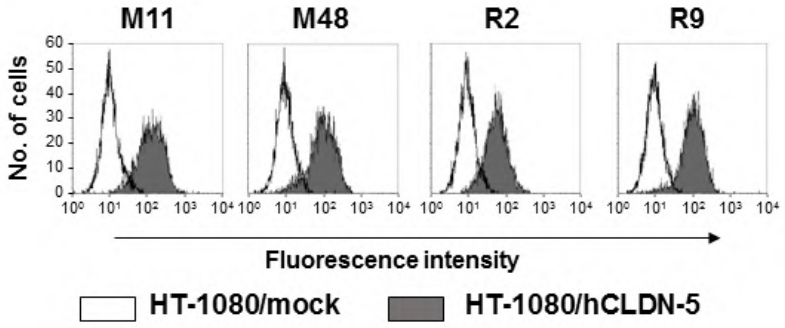

JPET Fast Forward. Published on August 17, 2017 as DOI: 10.1124/jpet.117.243014
This article has not been copyedited and formatted. The final version may differ from this version.

Figure 1.

B.

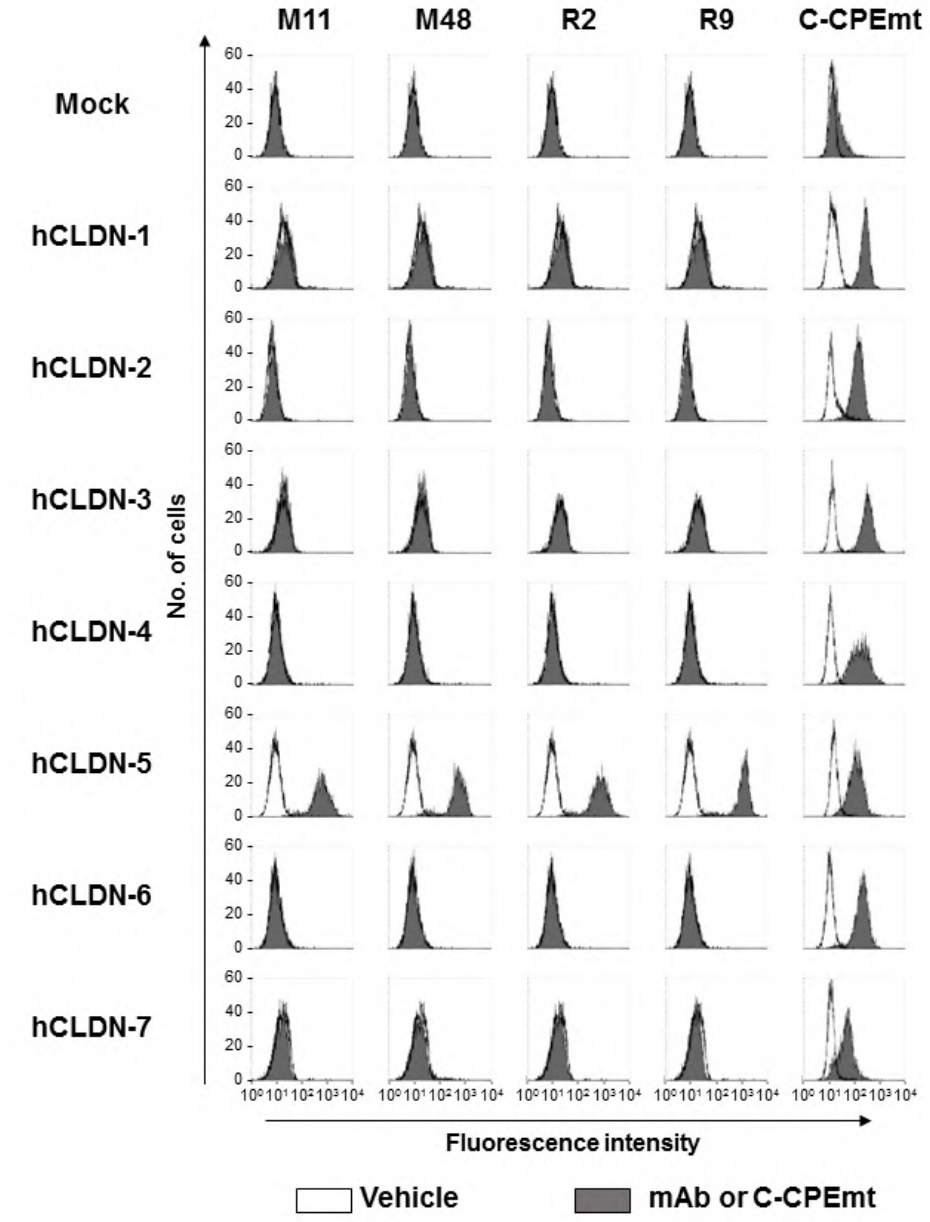

JPET Fast Forward. Published on August 17, 2017 as DOI: 10.1124/jpet.117.243014
This article has not been copyedited and formatted. The final version may differ from this version.

Figure 1.

C.

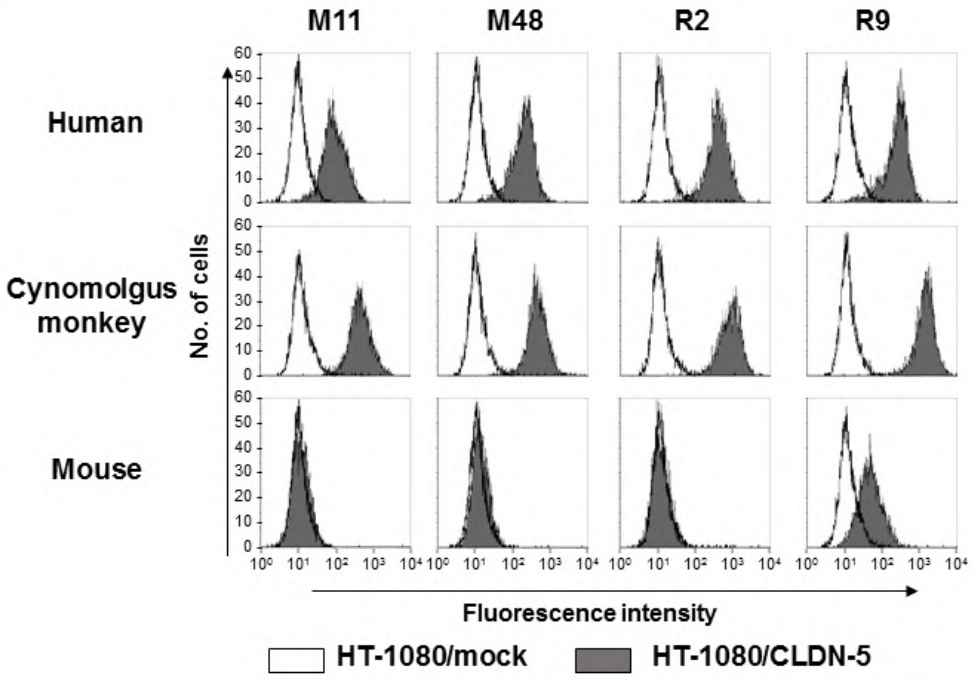

JPET Fast Forward. Published on August 17, 2017 as DOI: 10.1124/jpet.117.243014
This article has not been copyedited and formatted. The final version may differ from this version.

Figure 2.

A.

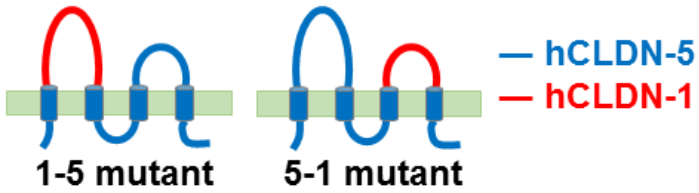

JPET Fast Forward. Published on August 17, 2017 as DOI: 10.1124/jpet.117.243014
This article has not been copyedited and formatted. The final version may differ from this version.

Figure 2.

B.

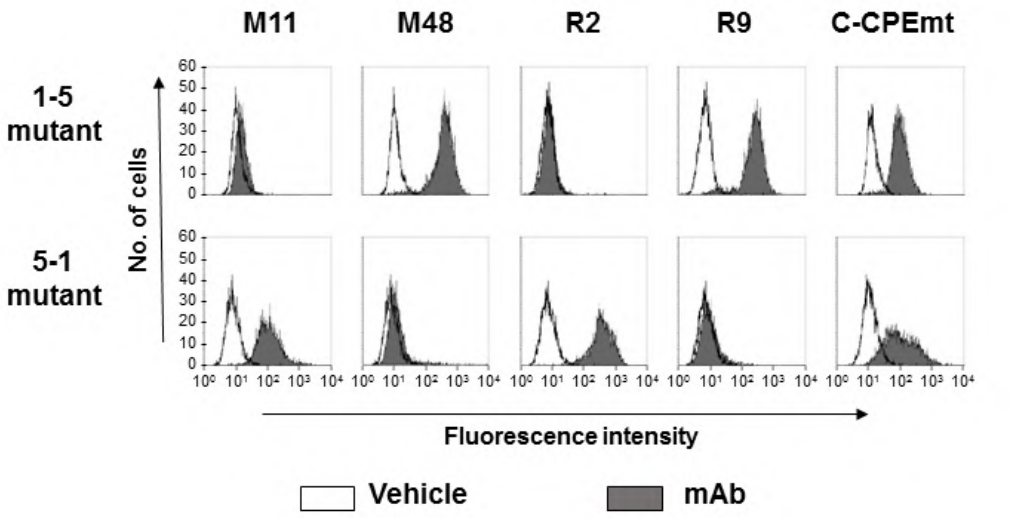

JPET Fast Forward. Published on August 17, 2017 as DOI: 10.1124/jpet.117.243014
This article has not been copyedited and formatted. The final version may differ from this version.

Figure 2.

C.

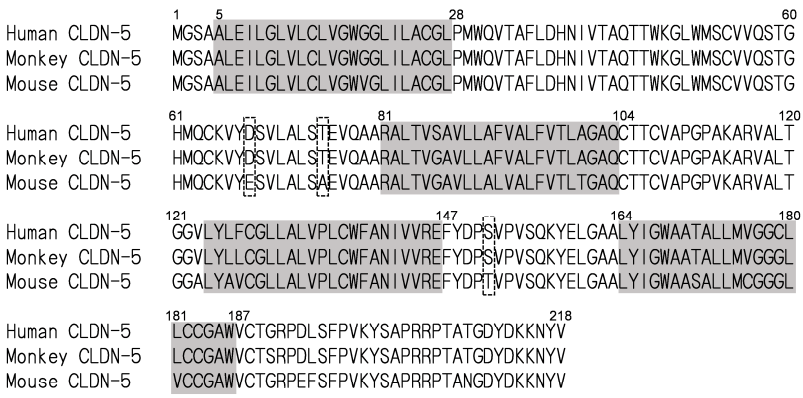

JPET Fast Forward. Published on August 17, 2017 as DOI: 10.1124/jpet.117.243014
This article has not been copyedited and formatted. The final version may differ from this version.

Figure 2.

D.

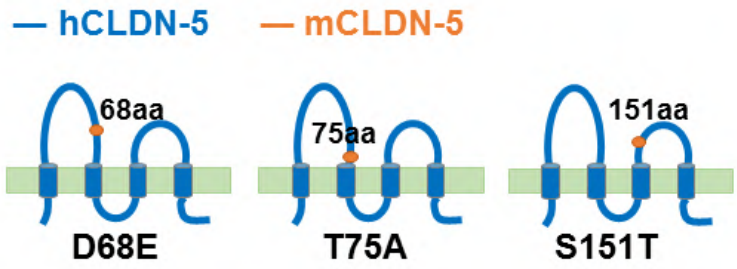

JPET Fast Forward. Published on August 17, 2017 as DOI: 10.1124/jpet.117.243014
This article has not been copyedited and formatted. The final version may differ from this version.

Figure 2.

E.

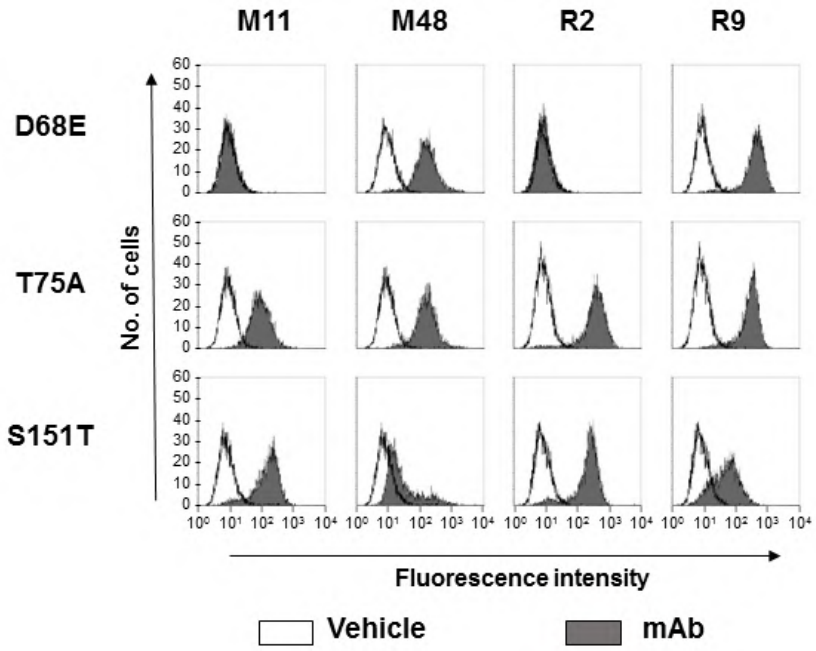

JPET Fast Forward. Published on August 17, 2017 as DOI: 10.1124/jpet.117.243014
This article has not been copyedited and formatted. The final version may differ from this version.

Figure 3.

A.

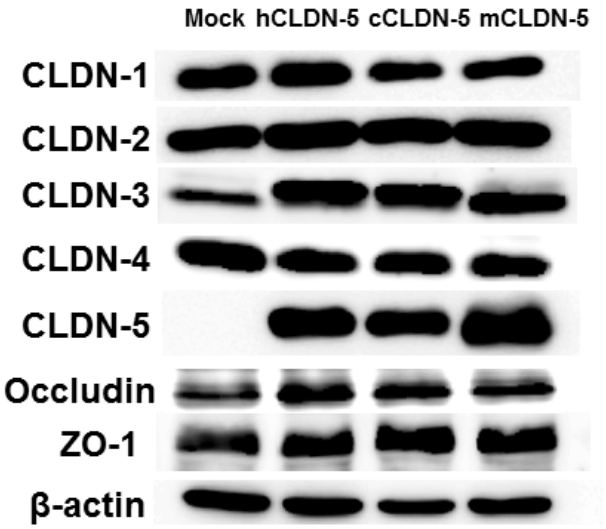

JPET Fast Forward. Published on August 17, 2017 as DOI: 10.1124/jpet.117.243014
This article has not been copyedited and formatted. The final version may differ from this version.

Figure 3.

B.

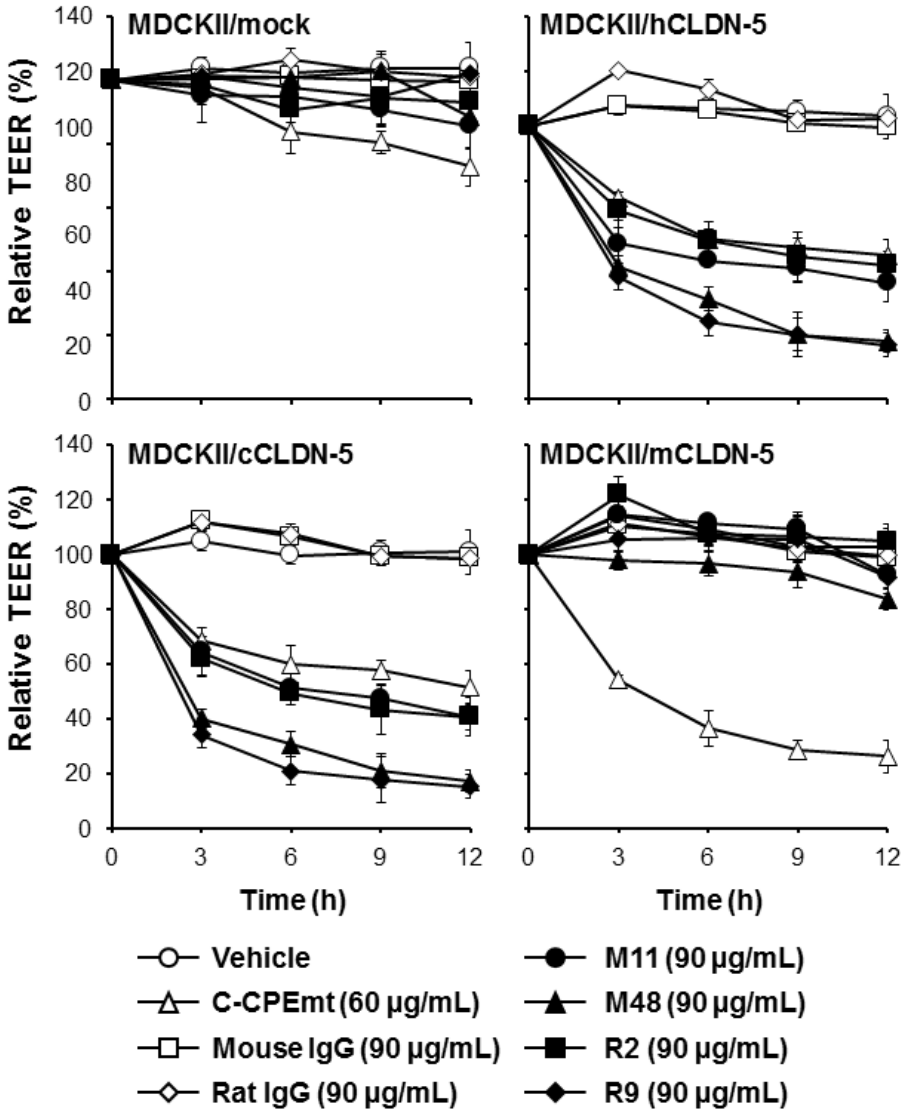

JPET Fast Forward. Published on August 17, 2017 as DOI: 10.1124/jpet.117.243014
This article has not been copyedited and formatted. The final version may differ from this version.

Figure 4.

A.

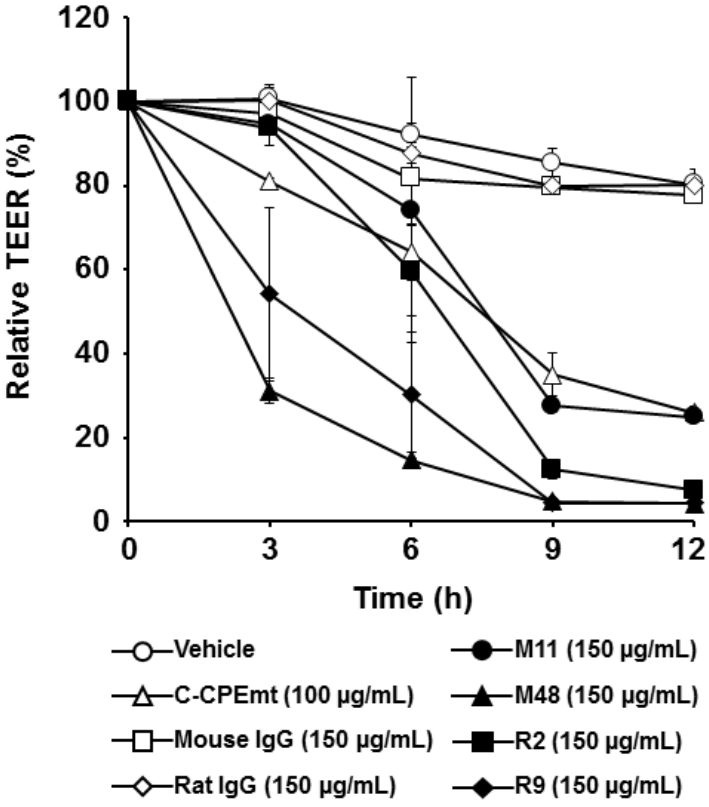

JPET Fast Forward. Published on August 17, 2017 as DOI: 10.1124/jpet.117.243014
This article has not been copyedited and formatted. The final version may differ from this version.

Figure 4.

B.

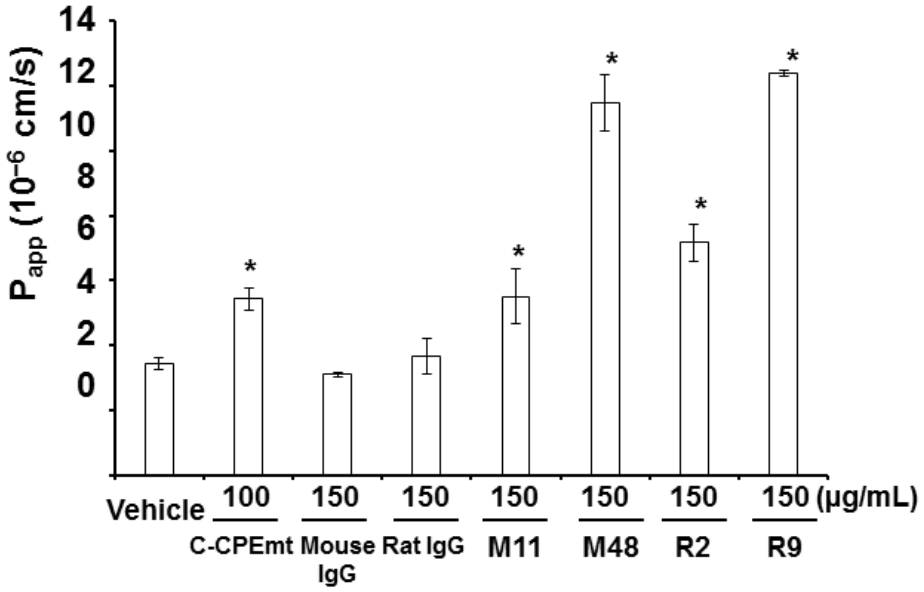

C.

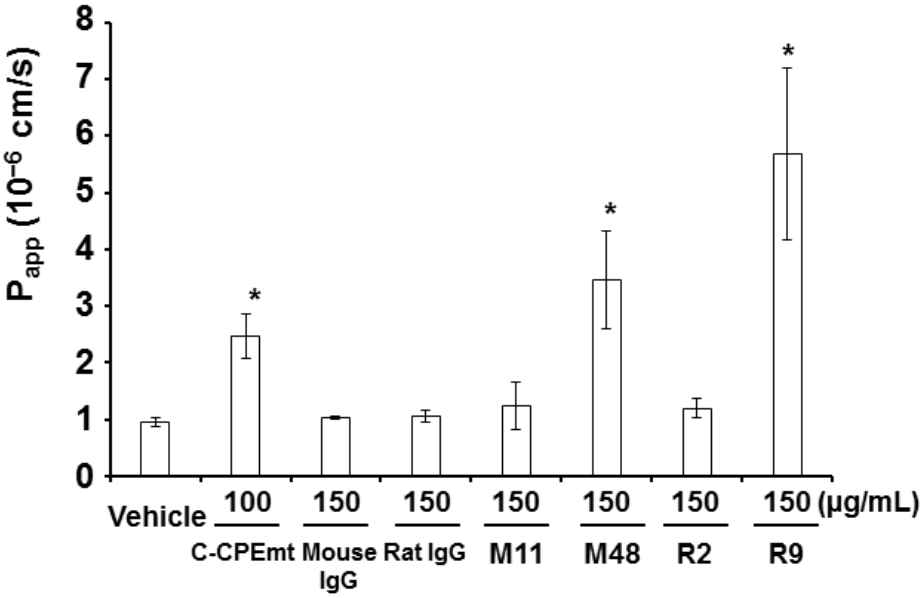

JPET Fast Forward. Published on August 17, 2017 as DOI: 10.1124/jpet.117.243014
This article has not been copyedited and formatted. The final version may differ from this version.

Figure 5.

A.

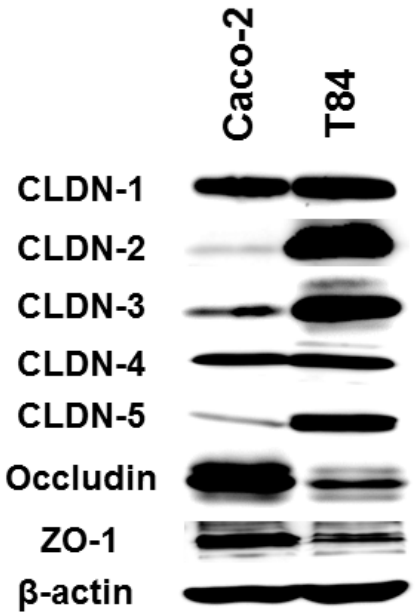

JPET Fast Forward. Published on August 17, 2017 as DOI: 10.1124/jpet.117.243014
This article has not been copyedited and formatted. The final version may differ from this version.

Figure 5.

B.